Constraints on ancient Mars atmospheric pressure and surface weathering processes from modeling and analysis of ancient impact crater populations

For submission to ROSES –Solar System Workings 2017 (NNH17ZDA001N-SSW)

2. Scientific/Technical/Management:

2.1 Summary. Despite the recent upsurge in data and analyses for the geologic record of early Mars wet climates, many key parameters remain poorly constrained. These include the pressure of the CO_2-dominated atmosphere, P_{atm}; surface temperature, T_{surf}; and the duration of the wet climates, τ_{wet}. P_{atm} is a key input for models of climate and atmospheric evolution (Haberle et al. 2017); T_{surf} has implications for both habitability and climate models (Vasavada 2017); and determining τ_{wet} is crucial for understanding Mars' habitability and Mars' utility as a benchmark for exoplanets (Ehlmann et al. 2016). **Despite the central importance of P_{atm}, T_{surf}, and τ_{wet}, direct constraints on these parameters are few (Wordsworth et al. 2016). Most existing methods have degeneracies.** For example, because clay-mineral formation proceeds faster under warm conditions, clay-mineral constraints on weathering processes record a convolution of time and temperature (the time-temperature integral; Tosca et al. 2009, Bishop et al. 2018) rather than constraining either parameter directly. In order to obtain improved constraints on these key parameters, we will apply our existing method making use of embedded (= syn-depositional, ancient) craters (Kite et al. 2013, 2014, 2017; Fig. 1), improving our existing models (Williams et al. 2014, Reed et al. 1998).

Specifically, we will first improve our model of impactor-atmosphere interactions to obtain the size-frequency distribution of small embedded craters in order to **retrieve Mars atmospheric pressure versus time** using 4 deposits of known relative age. In previous work we have interpreted the atmospheric pressure fits as upper limits. This approach **complements the estimate that may be obtained from MAVEN-era loss rates,** extrapolated back into the past. Second, we will apply our existing method relating embedded crater density to paleo-sedimentation rate for an exceptionally smectite-rich sedimentary deposit at Mawrth; this site is the oldest known sedimentary sequence in the Solar System (Loizeau et al. 2012), and an anchor for interpretations of Early Mars climate (Bishop et al. 2018). We shall thus obtain a *chronometry* for paleo-sedimentation rate – **the duration over which the Mawrth smectite-rich materials were built up**. Finally, we will combine our chronometry for Mawrth paleo-sedimentation with existing mineralogical constraints on Mawrth temperature-time integrals and existing models in a new framework (Fig. 4) to **break the temperature-time degeneracy** and **thus improve constraints on early Mars surface temperature during the Middle Noachian**. Thus, the proposed work will use modeling of a single observation – embedded craters – in order to provide improved constraints on the atmospheric pressure, and surface temperature, of early Mars.
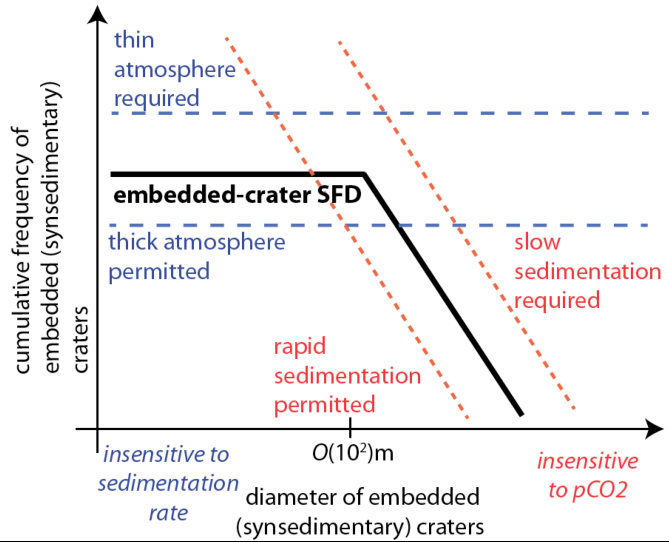

Fig. 1. Schematic diagram to show how modeling of the effects of paleo-atmospheric pressure and sedimentation rate on embedded-crater size-frequency distributions (blue dashed lines and red dashed lines respectively) allows both P_{atm} and sedimentation rate to be constrained by an embedded-crater size-frequency distribution (SFD) (thick black line) (Kite et al. 2013, 2014, 2017).

2.2 Goal of the proposed study.

The goal of the proposed work is to obtain new constraints on early Mars atmospheric pressure versus time and on the timescale and surface temperature for surface weathering processes (e.g., pedogenesis) on early Mars. Achieving this goal involves the following objectives:-

• Task 1: Improve existing model of atmosphere-impactor interactions; apply improved model to measured embedded-crater size frequency distributions at four sites of known relative age in order to constrain atmospheric pressure versus time (§2.4.1). Synthesize and compare to other observations;
• Task 2a: Constrain paleo-accumulation rate of sediments by modeling embedded-crater size-frequency-distribution for a 150m-thick smectite-rich sedimentary deposit at Mawrth, obtaining timescale (§2.4.2);
• Task 2b: Use chronometry from Task 2a to model surface weathering processes using a novel framework combining sedimentation dynamics and kinetics in order to constrain temperature (§2.4.3).

In order to define a focused, well-posed investigation of appropriate scope for a three-year study, we make several simplifying assumptions, which are explained and justified in §2.4.4.

2.3 Scientific background.

2.3.1. *The problem:* **Early Mars environmental evolution remains unclear, in large part because constraints on paleopressure and surface weathering processes are limited.**

Paleopressure: Atmospheric pressure versus geologic time for Mars has been a key unknown for over 40 years (e.g. Pepin 1994, Jakosky & Phillips 2001, Catling 2009, Haberle et al. 2017). It is believed that the atmosphere was CO_2-dominated (so $P_{atm} \approx P_{CO2}$), and that P_{atm} was greater in the past. However, constraints on atmospheric pressure versus time for Mars are few (Fig. 2), and mostly indirect ("*" symbols in Fig. 2). A simple, direct method of constraining paleo-atmospheric pressure was proposed by Vasavada et al. (1993) and put into action by PI Kite and Collaborator Williams in 2014 (Kite et al. 2014). In this method, the minimum size of craters serves as a proxy for palaeopressure of planetary atmospheres, because thinner atmospheres permit smaller objects to reach the surface at high velocities and form craters (Kite et al. 2014). This is because planetary atmospheres brake, ablate and fragment small asteroids and comets, filtering out small high-velocity surface impacts and causing meteors/meteorites. Kite et al. 2014 obtained an upper limit of 0.9±0.1 bar at a single site (~3.6 Ga) using this technique. The potential of our technique is that the 40-year-old prediction of a connection between drying and atmospheric decay can be tested by, **as we propose to do here, applying the small crater technique to sedimentary deposits of different ages – ranging from Mawrth (the oldest known sedimentary sequence in the Solar System), through Meridiani, to relatively young deposits. This will yield a time series of constraints on the atmospheric pressure of early Mars, stratigraphically coordinated to the sedimentary record of Mars's great drying**. Why has this has not been done already? Although embedded craters are not uncommon within Mars sedimentary deposits (e.g. Fig. 4 in Grotzinger et al. 2011; Fig. 17 in Lewis & Aharonson 2014;

Fig. 26 in Anderson & Bell 2010), constraining atmospheric-pressure models is difficult with one data point per site (Chappelow & Golombek 2010). Sites with abundant embedded craters are hard to find. We have located a handful of such sites. We will apply a uniform procedure and improved model to the 4 sites shown in Table 1 and thus obtain a time series of Mars atmospheric pressure constraints. A strength of the ancient-craters method is that it is a direct probe of paleoatmospheric pressure (Vasavada et al. 1993): if everything breaks against us, our limits might be wrong by a factor of 2, but not 10. This contrasts with indirect methods, whose interpretation can be controversial. Examples include (a) $^{40}Ar/^{36}Ar$ analysis of ALH 84001, where experts do not agree on the sign of the paleopressure constraint (Kurosawa et al. 2018 vs. Cassata 2012 – points 4 and 8 in Fig. 2); and (b) mineralogy, where a Hesperian upper limit of Bristow et al. (2017) has been raised by a factor of 100 due to new experiments (Tosca et al. 2017). Even on Earth, 30 years of study of the relationship between pCO_2 and mineralogy for Archean paleosols have not yet led to consensus (Kanzaki & Murakami 2015).

Surface weathering processes: Mars'

Fig. 2. How the proposed retrieval fits in the context of existing constraints (most of them indirect, denoted by "*"). Black symbols show result of Kite et al. 2014. **The proposed work will use a direct method to constrain paleopressure at times bracketing the "great drying" of Mars** using four sites (red triangles). (1*) cosmochemical estimate; (2*) prehnite stability; (3*) carbonate Mg/Ca/Fe (van Berk et al. 2012); (4*) $^{40}Ar/^{36}Ar$ (Cassata et al. 2012); (5) bomb sag (Manga et al. 2012; $n = 1$ data point); (6) modern atmosphere; (7) modern atmosphere + buried CO_2 ice; (8) $^{40}Ar/^{36}Ar$ (Kurokawa et al. 2018); (9) modern escape-to-space extrapolated into past (Lillis et al. 2017, Brain et al. 2017). (10*) bedform wavelengths (Lapotre et al. 2016). Approximate and model-dependent implications for climate are shown by background colours. Chronology: Hartmann (2005).

largely basaltic surface (Edwards & Ehlmann 2014) shows outcrops of surface weathering profiles that are critical to understanding Early Mars climate. During the Noachian, widespread and perhaps global surface weathering processes (plausibly pedogenesis) altered a 1-200m thick near-surface layer on Mars (Carter et al. 2015; Bishop et al. 2008, 2013, 2018; Noe Dobrea et al. 2010, 2011). In contrast to the low-W/R crustal clays (Ehlmann et al. 2011), these likely formed at high W/R from a basaltic protolith. Mawrth is the thickest and best-exposed record of this surface alteration event (e.g. Bibring et al. 2006, Bishop et al. 2013). Mawrth has a complex mineral stratigraphy (Fig. 3) recording multiple intercalated depositional episodes and top-down wetting events (Horgan et al. 2013, 2017a; Loizeau et al. 2015, Bishop et al. 2011, 2013, 2018). We focus on the thickest, most ancient layers, which are smectite-rich. The smectite-rich layers are draped onto regional topographic highs, strongly supporting a
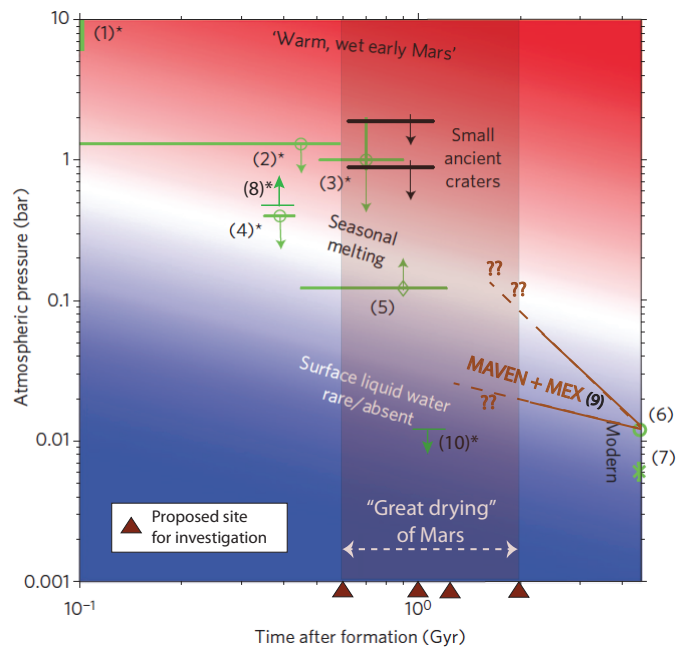
pedogenetic interpretation (Velde & Meunier 2008, Loizeau et al. 2012, Bishop et al. 2013). The thick smectites would imply rainfall and $T_{surf} \gtrsim 300K$ if we were to apply criteria that are standard on Earth (Velde 1995, Baker & Strawn 2014, Chadwick & Chorover 2010), broadly consistent with Mars ALH 84001 carbonate Δ^{47} (Halevy et al. 2011). Interestingly, such high temperatures would indicate that almost all existing models for Early Mars wet climates are incorrect, because they can only just reach 273K even with multiple optimistic assumptions (Wordsworth 2016). However, the case for high temperatures is not certain. Alternatives include alteration by cold low-pH fluids (modeled by e.g. Zolotov & Mironenko 2016, Peretyazhko et al. 2018), or very prolonged weathering at low temperatures (modeled by e.g. Fairén et al. 2011, Bishop et al. 2018). It is not possible to tackle this wide range of possible processes by Earth analogy alone, and so reaction-transport modeling is required (Fig. 4).
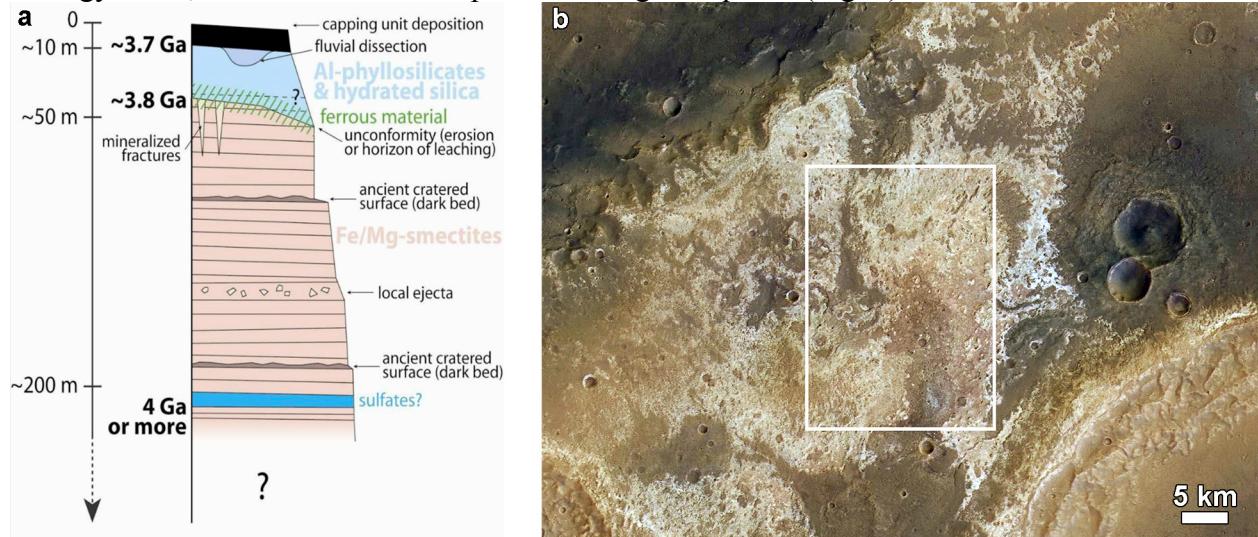

Fig. 3. (a) Mawrth Vallis mineral stratigraphy from Loizeau et al. (2012); Task 2 focuses on the layer marked 'Fe/Mg-smectites.' (b) HRSC color mosaic showing the focus area for Task 2, centered near ~24.4°N 21.2°W in the Mawrth region - the smectite-rich material is highlighted in the red/brown tones near the center of the rectangle.

Geochemical modeling for Mars near-surface processes is a large field (e.g. Catling 2009, Bulllock et al. 2004); we focus on modeling of the process most relevant at Mawrth, pedogenesis. For Mars pedogenesis, geochemical modeling has been carried out by many groups (e.g. Milliken et al. 2009, Zolotov & Mironenko 2016, Schieber et al. 2017), including kinetic factors calibrated against both terrestrial-analog observations and laboratory experiments. These methods clarify origin scenarios. However, existing work has two limitations. **The first, and most basic, barrier to progress is the temperature-time degeneracy.** This cannot be resolved by modeling alone, and more data on timescale is needed. A second barrier to progress is that no existing model considers wetting events intercalated with sediment deposition events, due to limitations in the reaction-transport codes. But this model limitation is in contradiction to terrestrial analogs (e.g. Retallack et al. 2000, Sheldon & Tabor 2009). It is also in contradiction to the numerous synsedimentary impact craters in Mawrth that show that sediment input was extended over a long time period. **We propose to vault both barriers** (Fig. 4).
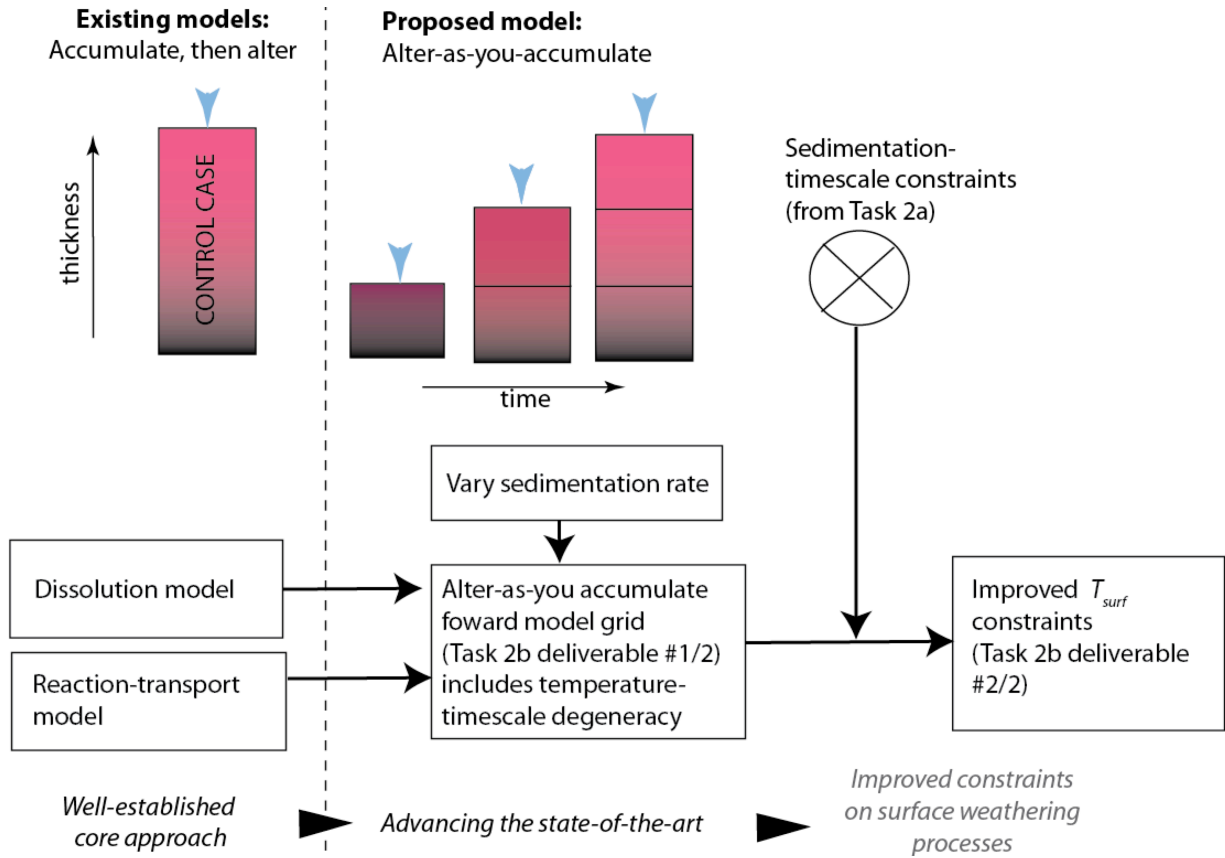
Fig. 4. Plan for improved modeling of Mars surface weathering processes. The core of our approach – the dissolution model and the R-T model – is shared with previous models (Fig. 5). The new element – sedimentation-timescale constraints – uses a previously published approach (Kite et al. 2013, 2017). The novelty of the approach is to combine these two well-established methods. Blue arrows correspond to top-down fluid input, favored by geologic context for the Mawrth smectites. A sequence of paleosols too closely-spaced to be resolved from orbit (which we refer to as 'alter-as-you-accumulate') is strongly favored by geologic evidence (e.g. Bishop et al. 2018, Retallack et al. 2000), but has not been previously modeled.

2.3.2. *Proposed solution:* **Numerical methods for atmosphere-impactor interactions, and for surface weathering, have advanced to the point that we can tackle both of these problems. Risk has been mitigated via our peer-reviewed publications.**

Risk has been mitigated via our peer-reviewed publications describing work that validates two of the three elements of our proposed technique.

Specifically, in Kite et al. 2014, we showed that the paleopressure model can provide interesting constraints at one site. Results are shown in Fig. 6 (and Fig. 2). Preliminary inspection suggests that the sites chosen for investigation in Task 1 (Table 1) will be no more challenging to model.

In Kite et al. 2013 and Kite et al. 2017, we showed that the sedimentation-rate estimation procedure can provide interesting constraints at multiple sites. Example results are shown in Fig. 8. Preliminary inspection suggests that the site chosen for investigation in Task 2 (Fig. 3) will be less challenging to model, due to the hi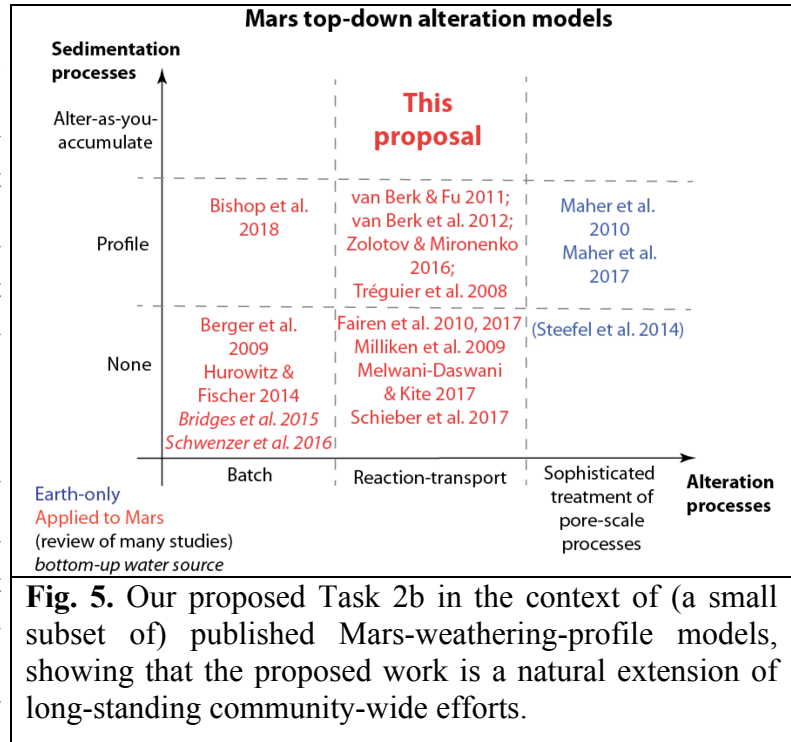gh abundance of embedded craters at the Task 2 site. The remaining element is reaction-transport modeling. For Earth work, it is now routine to relate clay

mineralogy to climate conditions (e.g Velde & Meunier 2008, Sheldon & Tabor 2009, Horgan et al. 2017b). On Earth, smectites are associated with annual average temperatures ~300K (rainfall) (e.g. Hobbs & Parish 2016). Modeling is needed to test the hypothesis of Mars smectite formation under cold conditions. Earth analogs are insufficient because Earth post-glacial timescales are insufficient for major smectite formation, and glaciation "wipes the slate" of soil formation (e.g. Lee et al. 2004). The exception proves the rule: it is clear that 240-250K mean annual temperatures are insufficient to form clays based on Antarctic Dry Valleys post-Miocene data. The Antarctic Dry Valleys largely lack pedogenic smectites (Bishop 2014, Gibson et al. 1983, Priscu et al. 1998). According to Berkley and Drake (1981) "Clay minerals are conspicuously sparse" in Antarctic Dry Valleys Drilling Project cores.[1] This mis-match between the Antarctic record and the mineralogical record at Mawrth is a challenge to cold-wet hypotheses for Early Mars (e.g., some versions of the Late Noachian Icy Highlands hypothesis; Fastook & Head 2015). Two possible resolutions are: (A) Early Mars really was warm (~300K) and wet (e.g., Craddock & Lorenz 2017); (B) the Mawrth record is exceedingly long-duration. **These hypotheses can only be tested using an independent measure of timescale, which we propose here (Task 2a).**

Despite the importance of multiple wetting events in forming accumulations of pedogenic soil profiles (e.g. McDonald & Busacca 1990), there has been little modeling effort expended on this idea. We will fix this by explicitly tracking alter-as-you-accumulate processes, in which many wetting events are intercalated with many sediment deposition events. Throughout this proposal, continuously-alter-as-you-accumulate is intended as an approximation that is appropriate to the interpretation of orbiter data for the smectite layer at Mawrth. At rover scale, we fully expect that the paleosol sequence will show discrete horizons, as on Earth (Retallack et al. 2000).

2.4 Technical Approach and Methodology.

Paleopressure is most strongly constrained by the smallest impact craters (Fig. 1), whereas the sedimentation rate is constrained by moderately large embedded impact craters (Fig. 1). Thus, Task 1 can advance independently of Task 2 because Task 1 involves fitting the *ratio* of small craters to large craters (not the absolute flux). Task 2 can proceed independently of Task 1 because sedimentation-rate fits rely on >200m-diameter embedded impact craters, whose abundance is much less affected by atmospheric filtering. Finally, Task 2b can proceed independently of Task 2a because

Fig. 5. Our proposed Task 2b in the context of (a small subset of) published Mars-weathering-profile models, showing that the proposed work is a natural extension of long-standing community-wide efforts.

---

[1] Laboratory timescales are also insufficient for high smectite yield (≈ concentrations) at low temperatures (Kloprogge et al. 1999, Baker & Strawn 2014).

Task 2b involves forward modeling of a look-up table for the dependence of smectite abundance on accumulation timescale, and Task 2a merely identifies a preferred "row" within that look-up table.

The proposed work requires 5 new HiRISE DTMs (Table 2). This will be done using the UChicago ASP Scripts (Kite & Mayer 2016), with which we have already generated 83 HiRISE DTMs. Based on this experience, we generously allocate 1 week for DTM production. 2/5 DTMs will be used only for Task 1, and 3/5 DTMs will be used for both Tasks 1 and 2. Embedded craters will be counted for each DTM. Examples of embedded impact craters are shown in Table 1. Cross-checking of our embedded-crater identifications is consistent with a false-positive rate of zero (Kite et al. 2014). This project will require inspection of 3 CRISM cubes (to be chosen from the 7 listed in Table 2) by the Co-I.

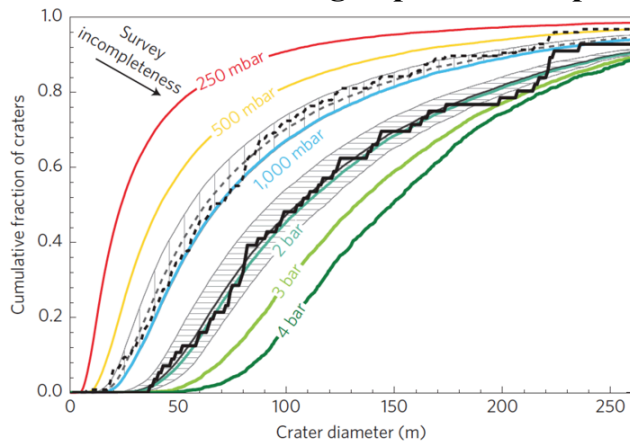## 2.4.1. Task 1: Modeling of paleo-atmospheric pressure using ancient impact craters.

Fig. 6. Comparison of model crater size–frequency distributions to observations at Aeolis Dorsa (from Kite et al. 2014). Solid black line corresponds to definite embedded craters. Dashed black line additionally includes rimmed circular mesas. Colored lines show model predictions for atmospheric filtering of small impactors at different pressures. Grey hatched regions correspond to 2-sigma statistical error envelopes around the best-fit palaeopressure to the data (best fits shown by thick grey lines). Survey incompleteness leads to overestimates of median crater size, so best fits are upper limits.

Paleopressure Model: The method for the paleopressure model is as follows (Paige et al. 2007, Kreslavsky 2011). Following Collaborator Williams et al. (2014, 2017) and Kite et al. (2014), we will build a synthetic impactor population by drawing randomly from a size distribution constrained by satellite observations, and an estimated initial-velocity distribution of meteoroids at Mars' orbit. Distributions of material types, densities, and ablation coefficients are set based on terrestrial fireball network observations (the model assumes the same fractional distribution at Mars) (Ceplecha et al. 1998). We advect these populations to the surface through atmospheres with scale height 10.7 km. The atmosphere drains kinetic energy from impactors via drag ($\propto$ velocity^2) and ablation ($\propto$ velocity^3). Particles braked to <500 m/s would not form hypervelocity craters and are removed from the simulation. Model output is not very sensitive to the details of how fragmentation is parameterized ($\lesssim$10%), nor to target density ($\lesssim$25% for range 1500-2500 kg/m^3), nor to reasonable variations in the mix of impactor strengths and densities. Crater sizes are calculated using π-group scaling (e.g. Holsapple et al. 1993), for which the most important uncertainty in this size range is target properties. Target properties are set based on facies analysis of the target rocks; in the worst case, facies-interpretation uncertainty can lead to a pressure uncertainty of up to a factor of 2 (Dundas et al. 2010, Collaborator Williams et al. 2017). We do not track secondary craters, because meter-sized endoatmospheric projectiles are likely to be braked to low speeds for the relatively thick atmospheres we are evaluating. In other

words, if wet-era small craters are secondaries, then early Mars' atmosphere was thin.[2] The size distribution of our synthetic impactor populations follows Brown et al. (2002); the initial-velocity distribution follows Davis (1993). Each population contains 3% irons, 29% chondrites, 33% carbonaceous chondrites, 26% cometary objects, and 9% "soft cometary" objects (following Ceplecha et al. 1998) with densities and ablation coefficients also set following Ceplecha et al. 1998. These settings will be altered for the proposed work, as described below. Fragmentation occurs when ram pressure exceeds disruption strength. Disruption strength is set to 250 kPa; much lower or much higher values would be inconsistent with the observation that more than half of craters observed to form in the current 6 mbar Martian atmosphere are clusters (Daubar et al. 2013). This strength is within the range reported for Earth fireballs (Ceplecha et al. 1998), and our model is insensitive to distruption-strength variations within the Ceplecha et al. (1998) range. We adopt an impactor entry angle distribution that peaks at 45°. The ratio of the final rim-to-rim diameter to the transient crater diameter is set to 1.3 (Melosh 1989). The excavation efficiency decreases as $1/(v \sin \theta_i)$ where θ_i is the impact angle (Pierazzo & Melosh, 2000). Finally, we limit the computational cost of the model by only injecting impactors at the top-of-the-atmosphere that are larger than a cutoff diameter. Up to 10^6 impactors are injected, as needed, to build up statistics. The best-fitting atmospheric pressure will be obtained by bayesian fitting of the normalized embedded-crater size-frequency distribution observations to cratering-model normalized size-frequency distribution output, treating the impacts as a Poisson process (Kite et al. 2014, Michael 2016, Wall & Jenkins 2012, Robbins et al. 2018). The normalization means that our results are insensitive to uncertainties in the ancient crater flux. Local-column atmospheric pressures will be corrected to the MOLA datum using site-averaged topography and assuming a scale height of 10 km. Because of unavoidable sampling bias in favor of larger craters, we interpret our best fits as upper limits (Kite et al. 2014, §2.4.4).

Fig. 7. (from Williams et al. 2014.) (a) Initial velocity versus final velocity, and (b) the ratio of initial and final projectile mass versus initial velocity, for a range of projectile diameters (10 cm – 1 m) where objects have properties of ordinary chondrites. Smaller faster objects are more effectively decelerated and ablated.

Paleopressure Model Improvements: We will make the following changes to the paleopressure model. (i) We will include improvements to knowledge of the size-frequency distribution of Mars-crossing objects (e.g. JeongAhn and Malhotra 2015). (ii) We will test the sensitivity of the model output to the alternative crater production function of Daubar et al. (2013). Applied to ancient craters, this will lead to a *lowering* of our upper limit. (iii) Currently, the code does not track planet curvature; we do not allow

---

[2] Early interpretations of HiRISE results suggested that unrecognized secondary craters significantly contribute to all counts of D < 1 km Martian craters (McEwen et al. 2006). However subsequent work, for example the synthesis by Hartmann & Daubar (2017), shows that once 'field secondaries' are included, the crater SFD of Hartmann (2005) remains valid over long timescales for small craters.

impactors to skip back to space. We will incorporate this effect, following Chappelow & Golombek (2010). (iv) We will include an "all irons" test case, corresponding to (hypothetically) stronger projectiles during the Late Heavy Bombardment. (v) Although our fiducial forward model will use the chronology function and crater production function of Hartmann (2005), we will also forward-model changes in the size distribution of impactors with time by extrapolating the model of Strom et al. (2005). We expect that change (v) will *reduce* our upper limits on paleoatmospheric pressure. Although collectively significant, we do not expect that these improvements will take long relative to the Task 2b code. This is because Collaborator Williams wrote the code, and PI Kite is experienced at making major changes to the code.
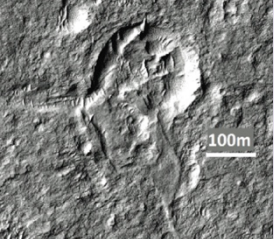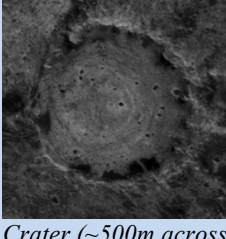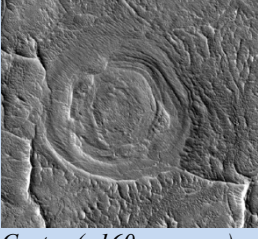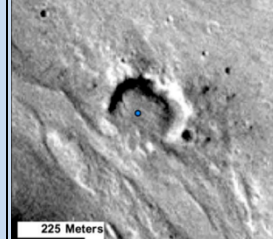
	Same Technique + Improved Method + 4 Sites Spanning A Wide Age Range			
Site	**SE Aeolis Dorsa (Kite et al. Nature Geoscience 2014)** [*Already published*]	**Mawrth (proposed)**	**East Meridiani, SW of Capen (proposed)**	**Alluvial fans in Margaritifer Terra (proposed)**
Example style of preservation	*Crater (240m across) interbedded with river deposits.*	*Crater (~500m across) was infilled by light-toned smectite-bearing sedimentary rocks*	*Crater (~160m across) was infilled by layered sediments, now forms outlier*	*Crater crosscut by fluvial trough; now backfilled by fan deposits.*
Geologic context	Inverted river channels Layered sedimentary rocks (Kite et al. 2014)	Phyllosilicates, some inverted channels (Noe Dobrea et al. 2010). Embedded craters at multiple levels.	Inverted river channels Layered sedimentary rocks (Hynek & di Achille 2017)	Alluvial fans (Grant & Wilson 2011, Kite et al. 2017b)
HiRISE stereopairs *(new DTMs italicized)*	ESP_019104_1740/ ESP_017548_1740; PSP_007474_1745/ ESP_024497_1745.	*ESP_023633_2050/ ESP_023343_2050; ESP_016394_2045/ PSP_008245_2045; PSP_004329_2045/ ESP_013282_2045.*	*ESP_021654_1855/ ESP_031212_1855; ESP_022221_1850/ ESP_039667_1850.*	Crater catalog already generated (Kite et al. 2017b)
Age (source)	**Noachian-Hesperian transition** (Kite et al. 2014).	**Middle Noachian** for selected strata (Loizeau et al. 2012)	**Early Hesperian** for selected DTMs (Hynek & di Achille 2017)	**Late Hesperian - Early Amazonian** (Grant & Wilson 2011)
Model used, paleopressure inferred	*Old model:* ≤(0.9±0.1) bar (Kite et al. 2014)	*Using Improved Model:* T o B e D e t e r m i n e d B y T h e P r o p o s e d I n v e s t i g a t i o n		

Table 1: Sites selected for measurement of ancient crater size-frequency distributions. Note that the Mawrth site was previously reported by Loizeau et al. (2010).

Paleopressure Target Selection: Embedded (synsedimentary) craters are found in many Mars sedimentary rocks. However, a single bolide is hard to interpret (Chappelow & Golombek 2010). Therefore, the sites listed in Table 1 are chosen because of the large number of embedded craters found at each site, and because these sites span a range in age (Table 1). In addition to the site-specific ages referenced in Table 1, the wide range in ages for the selected sites is also confirmed by published global sedimentary correlations of Grotzinger & Milliken (2012) and Ehlmann et al.

(2011). Inspection of anaglyphs for the specific stereopairs selected (Table 1) show that all sites have good preservation of crater infill, making embedded-crater identification straightforward. At each site, embedded craters are found at multiple stratigraphic levels, and so cannot be secondaries resulting from a single secondary impact.

Synthesis of results and comparison to models: After synthesizing our results with other published constraints, we will interpret the combined dataset in terms of trends in Mars atmospheric evolution. Because many process-based models of Mars atmospheric evolution already exist (e.g. Mansfield, Kite, et al. in press; Hu et al. 2015; Manning et al. 2006), we will not attempt to add our own in the proposed study, but instead we will accept/reject existing models. To complement these process-based models, we will use a very simple process-agnostic model $dP/dt = k_1 \times \exp(-t/\tau_1) - k2 \times \exp(-t/\tau_2)$ and report what combinations of $\{k_1, \tau_1, k_2, \text{and} \tau_2\}$ can satisfy the constraints.

2.4.3. Task 2a: Modeling of chronometry for Mawrth sedimentation.

HiRISE stereopair	Co-located CRISM observations (1 to be used for each HiRISE pair)
ESP_023633_2050/ESP_023343_2050	0001FAAE, 00021E6D, 0001F340
PSP_004329_2045/ESP_013282_2045	0000672C
ESP_016394_2045/PSP_008245_2045	0000AA7D, 000109E0, 0037E41

Table 2. Specific stereopairs and collocated CRISM observations at the selected Mawrth site, to be used for Task 2. The pairs will also be used for part of the paleopressure analysis in Task 1.

Task 2 focuses on sedimentary deposits in the Mawrth area. Mawrth has many embedded craters, and because impactor flux has decreased over time, this is plausibly related to Mawrth's great age. We do have some chronological constraints on Mawrth (e.g. Loizeau et al. 2012), but no understanding of the timescale of sediment accumulation. The accumulation timescale sets an upper limit on the time available for alteration; Mawrth's smectites are too thick to represent a single top-down alteration event (Loizeau et al. 2015, Bishop et al. 2018). The key missing piece for understanding Mawrth is alteration timescale.
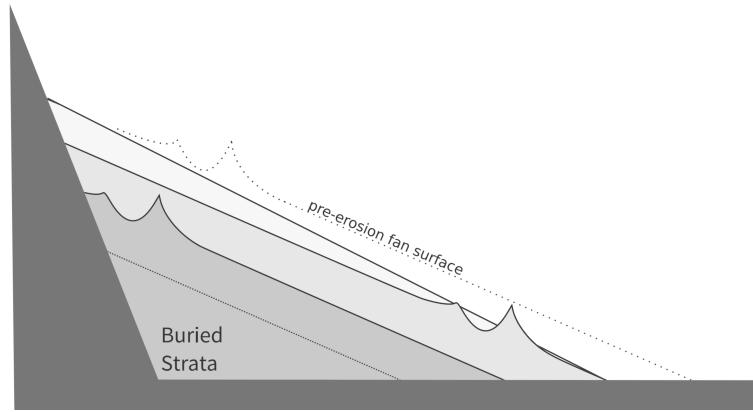
Fig. 8. Idealized cross section through a sedimentary deposit containing embedded craters (from a study of alluvial fans; Kite et al. 2017). Crater density within the sedimentary deposit may be estimated using the frequency of visible interbedded craters at the exposed surface. Even if postfluvial erosion was severe, the areal density of exposed embedded craters of a given diameter is still proportional to the volumetric density of those craters. Thus, a count of embedded craters constrains the deposit's aggradation rate.
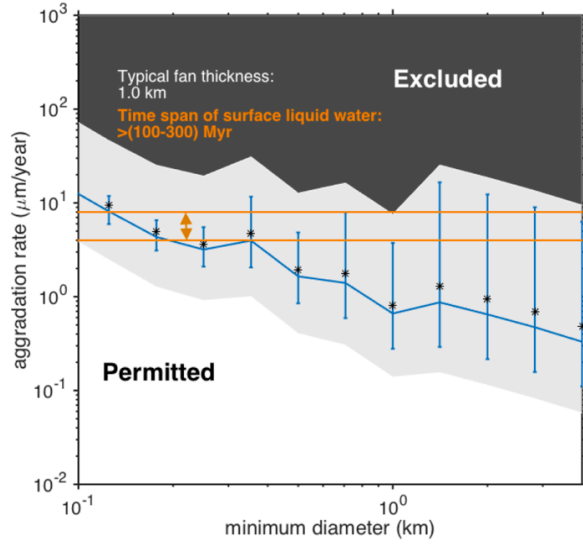
Fig. 9. Example of sedimentation-rate estimation, from a study of alluvial fans (Kite et al. 2017). Embedded-crater data binned by minimum diameter (cumulative plot). Blue error bars bracket the 90% confidence intervals on lower limit (by Poisson estimation). Full Monte Carlo fit corresponds to the gray band. Black zone is excluded with >95% confidence. White zone is excluded in <5% of trials. Black asterisks correspond to the median outcome of the Monte Carlo procedure. Orange lines and associated τ_{wet} constraints assume a steady aggradation rate.

We will obtain a sediment accumulation rate averaged over Mawrth smectite-layer thickness. To do this, we will use embedded-crater size-frequency distributions (Fig. 1). In our inversion, we propose a systematic scan through the following uncertainties, using a Monte Carlo approach (Fig. 9). The parameters to be varied are:- crater chronology function (Johnson et al. 2016); target strength; filtering by a potentially thicker past atmosphere; the central time of formation of the deposits (which affects crater flux); and the amount of burial or erosion (expressed as a fraction of the crater's diameter) that is needed to prevent the crater from being detected at HiRISE resolution. We will adopt conservative prior probabilities on these parameters in a Monte Carlo forward model of embedded-crater density. Specifically, we will assume (1) a factor-of-4 uncertainty in crater flux (log-uniform uncertainty between 0.3× and 3× the Michael et al. 2013 fluxes)[3]; (2) log-uniform uncertainty in target strength between limits of 65 kPa and 10 MPa (Dundas et al. 2010); (3) log-uniform uncertainty in paleo-atmospheric pressure between limits of 6 mbar and 1000 mbar (updated with the 2σ upper limit obtained from Task 1); (4) a uniform uncertainty between the range of published ages for Mawrth smectite-layer sediment deposition (3.9 - 3.7 Ga; Loizeau et al. 2012) and (5) a log-uniform prior for obliteration depth fraction (expressed as a fraction of diameter) from 0.05 (rim burial; Melosh 1989) to 0.2 (original crater depth; Watters et al. 2015). For each Monte Carlo trial, the effect of Poisson error is calculated analytically. Given the observations and the randomly-sampled parameters, each Monte Carlo trial yields an analytic probability for each candidate age (or each candidate aggradation rate) in each size bin. These probabilities are averaged over 10^3 Monte Carlo trials (Fig. 9). Embedded crater size-frequency distributions have a shallower size-frequency distribution than the crater production function, due to geometric effects (e.g. Lewis & Aharonson 2014), by 1.0 units on a log-log plot. This provides an internal cross-check on the results because any false positives (i.e., post-depositional, modern-era craters incorrectly classified as embedded) will rotate the SFD towards production. Our crater count areas are ~10^2 km², and we get good statistics. Yet Warner et al. (2015) showed that count area >10^3 km² is required for crater chronology. This apparent contradiction can be resolved by noting that rate-measuring (chronometry) studies have prior uncertainties that span many orders of magnitude more prior uncertainty than for chronology

---

[3] Even lower fluxes are possible (Bottke & Andrews-Hanna 2017), but this range is conservative for the purposes of setting a lower bound on the accumulation time for Mawrth.

11

studies. This washes out the error sources identified by Warner et al. (2015). Finally, we will test steady vs. unsteady accumulation hypotheses. While in detail sedimentation is always unsteady (e.g. seasonal dust-storms), when averaged over long timescales, Mars sedimentation can be steady (e.g. Lewis et al. 2008). We will test the following end-member hypotheses: (1) All embeds formed at a single stratigraphic layer (unsteady). (2) Embeds formed at a constant flux (craters / m^2 / column m) during sediment build-up. In order to carry out these tests, we will tag each embedded crater with a best-fit stratigraphic elevation, measured using our HiRISE DTMs relative to a local marker bed. Marker bed examples from a site elsewhere in the Mawrth deposit are shown in Fig. 13 of Loizeau et al. 2015. The main output from Task 2a will be an accumulation timescale, with uncertainty, for the Mawrth deposits.

2.4.3. Task 2b: Improved Mawrth surface-weathering models using chronometric constraints.

In principle a top-down alteration stratigraphy can be produced by a single climate event (Zolotov & Mironenko 2016). However, Mawrth geology records multiple, discrete, top-down aqueous alteration events (Bishop & Rempe 2016, Loizeau et al. 2015). We will model formation and alteration of the oldest part of the stratigraphy, the >150m-thick smectites, by multiple, discrete, top-down aqueous alteration events. Smectite formation can be explained by either brief warm climates, or exceedingly long alteration at low temperature – a time-temperature degeneracy (Bishop et al. 2018).

Using our chronometry from Task 2a and CHIM-XPT, we will model 2 end-member scenarios, the "control" and "alter as you accumulate" cases shown in Fig. 4. We will use the CHIM-XPT reaction-transport code (Reed et al. 1998, Melwani Daswani & Kite 2017, Kite & Ford 2018). As in Melwani Daswani & Kite (2017) and Kite & Ford (2018), we will use the updated thermodynamic database SolthermBRGM, which includes data for low-temperature geochemistry from the BRGM Thermoddem database (Blanc et al. 2012) among other sources. Book-keeping for minerals and aqueous species abundances during multi-layer accumulation-during-alteration is complicated. To handle this book-keeping, we will break the problem into 2 parts: reaction-transport calculations for each layer at each time-step, to be done in CHIM-XPT; and book-keeping for material supply by dissolution of not-yet-altered minerals plus down-column transport of aqueous fluids, to be done in MATLAB. A MATLAB control script will initiate CHIM-XPT runs. The input rock content for CHIM-XPT calculations will be set by dissolving protolith (±any secondary minerals) according to phase-dependent dissolution rates using MATLAB, and updating the CHIM-XPT input file accordingly (Milliken et al. 2009). We will bracket mineral dissolution-rate uncertainties by using the T-dependent rates from Brantley & Olson (2014, their Tables 3 and 5) and White & Buss (2014, their Table 4). Any given CHIM-XPT run will only have "visibility" of a single regolith layer, and the updating of fluid and rock compositions will be done in MATLAB via parsing of the CHIM-XPT output files and editing of CHIM-XPT input files[4]. With the MATLAB wrappers, this is a reaction-transport model even though CHIM-XPT will (in effect) be used in batch mode. For each scenario, we will assume protolith with the elemental composition of Rocknest soil (Blake et al. 2013), corrected for Cl (as NaCl) and S as ($MgSO_4$) (Siebach et al. 2017). Effective grain sizes (= reactive surface areas) will be taken from a terrestrial analog, specifically the John Day Fossil Beds (Retallack 2000). Sensitivity tests for grain sizes 10× larger and 10× smaller will be carried out for (2×)4 selected

---

[4] The PI has completed a conceptually similar MATLAB + CHIM-XPT project (Kite & Ford 2018).

runs. Mineral composition will be from Rocknest XRD (Bish et al. 2013), using SAM EGA for the S-bearing phases (McAdam et al. 2014). To minimize dust contributions, amorphous/short-range-order-phase composition will be from Sheepbed mudstone XRD (Dehouck et al. 2014). While other protoliths are possible, basalt is very common on Mars (Edwards & Ehlmann 2014). The input fluid shall be H_2O equilibrated with a CO_2 atmosphere with an O_2/CO_2 ratio equal to the present value; both 0.1 bar and 1 bar pCO_2 will be considered. Two aqueous-S input cases (Farrand et al. 2014, Peretyazhko et al. 2018) will be considered; (1) zero SO_2; and (2) waters equilibrated with 10 ppm SO_2. The range of T_{surf} for the reactions and the dissolution-rate calculations will be 0.1°C, 20°C, and 40°C. 20°C is selected to be consistent with ALH 84001 Δ^{47} (Halevy et al. 2011), and 40°C is selected as the hottest temperature for subaerial smectite formation on Earth. The soil will be divided into layers of thickness 3 m, and sediment will accrete in 3 m-increments as the calculation continues, up to a maximum of 50 layers (Fig. 4). The total thickness modeled, 150 m, is set to match observations (Loizeau et al. 2012). The increment thickness is chosen for numerical convenience, and also because the paleosol sequence is likely to consists of discrete horizons based on Earth analogy. Fluids from each layer will have pH raised by reaction with surface rocks, and then infiltrate to lower layers. The percentage of water that is removed (by assumption, routed to surface runoff or evaporation) at each 3 m-depth infiltration step will be varied {0%, 50%, 99%}. The uppermost value takes account of decreased porosity due to illuviation of clays. The accumulation rate will be varied, with 10-fold steps, between 10 nm/yr to 10 mm/yr. Bash wrapper scripts and MATLAB control scripts will be written to edit CHIM files to reflect the results of calculations in other layers. Solid solutions will initially be suppressed (with only end-member compositions included) because runs with solid solution require too much human intervention to be used in a CHIM-XPT grid scan. Sensitivity tests for inclusion of solid solutions will be carried out for 10 selected runs. An initial porosity of 0.3 will be assumed. This will be allowed to evolve as calculation proceeds; we will test the sensitivity of the results to the constant-porosity alternative. Rain/snowmelt rates from 0.01-10 m/yr will be considered in flushing calculations. This range brackets hyperarid through post-basin-forming-impact "rainout" conditions. We note that the highest rates imply an energetically unsustainable planetary energy balance, and are unfavorable for smectite formation (Eberl 1984); we will highlight the energetically unsustainable range in our published figures. Seasonality will not be explicitly modeled, but can be introduced in the analysis by a multiplicative factor. Mineral dissolution will be modeled as a function of time (not rain/snowmelt supply). The parameters to be varied lead to a total of 2 mineral-dissolution rates × 3 temperatures × 3 fluid-rerouting assumptions × 2 SO_2 cases × 7 accumulation timescales × 5 rain rates × 50 accumulation steps × an average of 25 layers = 1.6×10^6 runs. Each run takes <10 minutes on 1 core, so the ensemble can easily be run on the PI's cluster. Alternatively, we have access to dedicated nodes on a parallel cluster at the University of Chicago.

The smectite abundances in our ensemble of forward models (a total of 2 × 3 × 3 × 2 × 7 × 5 = 1260 forward models) will then be compared to Mawrth smectite abundances estimated from VNIR and TIR spectroscopy (e.g. Bishop et al. 2018, and references therein), using the accumulation timescales obtained from Step 2a. It is unlikely that the accumulation timescale from Task 2a will fall outside the range in the forward-modeled grid from Task 2b, but if it does, then it wil be straightforward and computationally inexpensive to add the appropriate 'plane' to the look-up grid corresponding to the Task-2a-output accumulation timescale. We will discuss the geologic reasonableness of the parameter combinations that are consistent with data. We will report the lowest-T solutions consistent with data, for each combination of SO_2 case, mineral-

dissolution rate, and fluid-rerouting assumption. Thus, the results from from Step 2b will either reinforce, or remove, the tension between climate models and mineralogy at Mawrth.

2.4.4. Assumptions and caveats.

It is worth emphasizing the limitations and assumptions of these modeling methods. First, this is a model-driven proposal whose primary goal is improved constraints on atmospheric pressure and surface weathering processes on early Mars. As with terrestrial paleoclimate research, a complete understanding of Mars' long-term climate evolution will require input from extensive data analysis, sample analysis including isotopes, and laboratory studies, all of which require equipment and personnel beyond the scope of a single Solar System Workings proposal. Second, a caveat with the paleopressure method is that we could be measuring periods of atmospheric collapse (Soto et al. 2015, Kite et al. 2017). However, global circulation models indicate that the total (atmosphere + ice-caps) CO_2 inventory must be ≤ 1 bar for atmospheric collapse (Soto et al. 2015, Forget et al. 2013). So, even if our measurements probe atmospheric collapse, as is possible, then that would still imply a low total CO_2 inventory, and thus a low *inflated* atmospheric pressure. Another issue is that our best fits are upper limits on paleopressure and sedimentation rate; we cannot rule out the possibility that small craters existed, but were obliterated by diffusion (Golombek et al. 2014) or other erosion processes (Jerolmack & Paola 2010). Therefore, our paleopressure method is not a panacea; rather, it instead complements other methods that provide lower limits, such as the bomb sag method (Manga et al. 2012). One potential uncertainty with Mawrth modeling is the lab-to-field correction for reaction kinetics. However, recent rapid progress on pedogenesis modeling for Earth indicates that pore-fluid-flushing is the key limiting process on weathering and largely accounts for the lab-to-field discrepancy (Brantley & Olson 2014, Maher et al. 2014, Winnick & Maher 2018). Because pore-fluid flushing is explicitly accounted for in CHIM, our results should account for this uncertainty. To mitigate remaining uncertainty, we will also report results for 10× slower and 100× slower kinetics. A second Mawrth uncertainty is that we cannot exclude the possibility that the sediments were built up over a long time and then swiftly altered at higher temperatures. This is unlikely, because terrestrial analogs strongly favor the alter-as-you-accumulate option, which is the preferred interpretation of all Mawrth specialists (reviewed in Bishop et al. 2018). Nevertheless, by itself our modeling can only establish the plausibility of lower-temperature longer-duration alteration (or, alternatively, reject this hypothesis), and cannot by itself prove this scenario. Mawrth has a long and presumably complex history; we propose to use models to test simple hypotheses about that history, with an eye to enabling richer hypotheses and tests in future.

2.5. Perceived Impact of the Proposed Work.

The paleopressure method is complementary to noble gas studies, and also escape-relevant measurements from MAVEN. Mawrth is one of two finalists for the ExoMars rover landing site, and as Mawrth was highly ranked as a landing site for MSL and Mars 2020, it is a plausible future NASA landing site. Mawrth is important because it is the oldest known sedimentary sequence in the Solar System, and has great significance for Mars climate modeling is great (Bishop et al. 2018), so breaking the T_{surf} - τ_{wet} degeneracy at this site will be useful. Chronometry is a key uncertainty and is a MEPAG priority: Investigation A1.1 of the MEPAG Goals (MEPAG Goals Document 2015) calls for improved knowledge of "rates […] of weathering." This chronometry complements existing efforts to obtain an absolute *chronology,* which are vital, but have large error bars (e.g. Loizeau et al. 2012). The alter-as-you-accumulate forward model grid

can be applied to all Mars top-down weathering profiles, not only Mawrth. Mars climate models can just marginally achieve annually average temperatures ~270K (snowmelt). However, the further increase to 300K – as would be required to match simple interpretations of the smectites – requires a >50% increase in surface Outgoing Longwave Radiation, and this is unattainable with all published models. So, which is incorrect, the models or the data interpretation? Our proposed work will address this question, which has been referred to as "the great climate paradox of ancient Mars" (Hynek 2016). Finally, this work will both benefit from, and also inform, Co-I Horgan's work on cold-climate pedogenesis at Gale which is funded through her MSL Participating Scientist Program grant. The Relevance Statement for this proposal is included on the cover page as requested in Appendix C.3 of the NRA.

2.6. Work Plan.

	Activities/milestones.	Products.
Year 1.	• Count craters for the 2 new paleopressure sites. • Improve model of atmosphere-impactor interactions. • Apply newly-improved model to infer paleopressure. • Build DTMs for Mawrth.	✓ LPSC presentation on: Paleopressure results and model fits for the 2 new sites. ✓ GRL-length paper on paleopressure versus time including synthesis with results obtained by other methods.
Year 2.	• Count craters for Mawrth, one DTM only. • Initiate CHIM modeling, train student on CHIM. • Interpolate structure contours using CRISM mineralogy.	✓ LPSC presentation on: Chronometry of sediment accumulation at Mawrth. ✓ GRL-length paper on chronometry for Mawrth.
Year 3.	• Extend stratigraphic workflow to adjacent Mawrth DTMs. • Conclude CHIM modeling, with sensitivity tests and parameter sweeps for Mawrth. • Write up results.	✓ LPSC presentation on: Effect of adding new DTMs to Mawrth results. ✓ JGR-length paper with results from improved modeling for Mawrth, including details of Mawrth modeling.

Productivity on past SSW grants with Kite as PI is as follows:
NNX15AH98G, 3 papers submitted in 3 years; NNX16AG55G, 5 papers submitted in 2 years.

2.7. Personnel and Qualifications. (For FTE information, see §6 and §8).

PI **Edwin Kite** is an assistant professor at the University of Chicago (UChicago). As PI, he will participate in all aspects of the proposed work and oversee its implementation. He has been the lead author or PI for >20 Mars papers, including papers on the use of small embedded craters for paleopressure retrieval and as process chronometers. Co-I **Briony Horgan** is an assistant professor at Purdue University. She has extensive experience interpreting spectral signatures of aqueous alteration in Mars visible, near-infrared, and mid-infrared datasets as well as terrestrial analog sites. She will be responsible for the mineralogical input to the reaction-transport model, and will play a major role in the overall synthesis and interpretation of mineralogical/crater data with model output for Mawrth. Co-I Horgan will also assist with manuscript preparation in Years 2 and 3. Collaborator **Jean-Pierre Williams** is an Associate Researcher at UCLA. He will consult on the application and upgrading of his model of impactor-atmosphere interactions to the reconstruction of Mars atmospheric history, and the interpretation of the paleo-pressure results. Collaborator **Mark Reed** is a professor at the University of Oregon, and principal author of the CHIM-XPT code; within the last year, he has co-authored on 2 previous papers applying the CHIM-XPT code to Mars problems. He will consult on the application of his CHIM-XPT code. A **University of Chicago graduate student researcher** (to be identified) will carry out the CHIM-XPT modeling effort and the Mawrth stratigraphic analysis as part of their PhD research.

3. References.

Anderson, Ryan B.; Bell, James F., III, 2010, Geologic mapping and characterization of Gale Crater and implications for its potential as a Mars Science Laboratory landing site, International Journal of Mars Science and Exploration, vol. 4, p.76-128.

Bandfield, J.L., Glotch, T.D., Christensen, P.R., 2003. Spectroscopic identification of carbonate minerals in the martian dust. Science 301, 1084–1087.

Baker, V.R., et al., 1991, Ancient oceans, ice sheets and the hydrological cycle on Mars, Nature, 352, 589-594.

Baker, L. L. & Strawn, D. G. Temperature effects on the crystallinity of synthetic nontronite and implications for nontronite formation in Columbia River basalts. Clays Clay Miner. 62, 89–101 (2014).

Barabash, S. et al., 2007. Martian atmospheric erosion rates. Science 315, 501–503.

Berkley, J. L.; Drake, M. J., 1981, Weathering of Mars - Antarctic analog studies, Icarus, vol. 45, Jan. 1981, p. 231-249.

Bibring, Jean-Pierre; Langevin, Yves; Mustard, John F.; Poulet, François; Arvidson, Raymond; Gendrin, Aline; Gondet, Brigitte; Mangold, Nicolas; Pinet, P.; Forget, F.; OMEGA Team; Berthé, Michel; Gomez, Cécile; Jouglet, Denis; Soufflot, Alain; Vincendon, Mathieu; Combes, Michel; Drossart, Pierre; Encrenaz, Thérèse; Fouchet, Thierry; Merchiorri, Riccardo; Belluci, GianCarlo; Altieri, Francesca; Formisano, Vittorio; Capaccioni, Fabricio; Cerroni, Pricilla; Coradini, Angioletta; Fonti, Sergio; Korablev, Oleg; Kottsov, Volodia; Ignatiev, Nikolai; Moroz, Vassilli; Titov, Dimitri; Zasova, Ludmilla; Loiseau, Damien; Pinet, Patrick; Doute, Sylvain; Schmitt, Bernard; Sotin, Christophe; Hauber, Ernst; Hoffmann, Harald; Jaumann, Ralf; Keller, Uwe; Arvidson, Ray; Duxbury, Tom; Neukum, G., 2006, Global Mineralogical and Aqueous Mars History Derived from OMEGA/Mars Express Data, Science, Volume 312, Issue 5772, pp. 400-404 (2006).

Bish, D. L.; Blake, D. F.; Vaniman, D. T.; Chipera, S. J.; Morris, R. V.; Ming, D. W.; Treiman, A. H.; Sarrazin, P.; Morrison, S. M.; Downs, R. T.; Achilles, C. N.; Yen, A. S.; and >200 coauthors, 2013, X-ray Diffraction Results from Mars Science Laboratory: Mineralogy of Rocknest at Gale Crater, Science, Volume 341, Issue 6153, Special Issue, id. 1238932.

Bishop, Janice L.; Dobrea, Eldar Z. Noe; McKeown, Nancy K.; Parente, Mario; Ehlmann, Bethany L.; Michalski, Joseph R.; Milliken, Ralph E.; Poulet, Francois; Swayze, Gregg A.; Mustard, John F.; Murchie, Scott L.; Bibring, Jean-Pierre, 2008, Phyllosilicate Diversity and Past Aqueous Activity Revealed at Mawrth Vallis, Mars, Science, Volume 321, Issue 5890, pp. 830-

Bishop, Janice L.; Loizeau, Damien; McKeown, Nancy K.; Saper, Lee; Dyar, M. Darby; Des Marais, David J.; Parente, Mario; Murchie, Scott L., 2013, What the ancient phyllosilicates at Mawrth Vallis can tell us about possible habitability on early Mars, Planetary and Space Science, Volume 86, p. 130-149.

Bishop, Janice L., Peter A. J. Englert, Shital Patel, Daniela Tirsch, Alex J. Roy, Christian Koeberl, Ute Böttger, Franziska Hanke, Ralf Jaumann, 2014, Mineralogical analyses of surface sediments in the Antarctic Dry Valleys: coordinated analyses of Raman spectra, reflectance spectra and elemental abundances, published 3 November 2014.DOI: 10.1098/rsta.2014.0198

Bishop, Janice L., Alberto G. Fairén, Joseph R. Michalski, Luis Gago-Duport, Leslie L. Baker, Michael A. Velbel, Christoph Gross and Elizabeth B. Rampe, 2018, Surface clay

formation during short-term warmer and wetter conditions on a largely cold ancient Mars, Nature Astronomy, https://doi.org/10.1038/s41550-017-0377-9

Blanca,Ph, A.,Lassina,P.Piantonea,M.Azarouala,N.Jacquemet,A.Fabbric, & E.C.,Gaucherd, 2012, Thermoddem: A geochemical database focused on low temperature water/rock interactions and waste materials, Applied Geochemistry, Volume 27, Issue 10, October 2012, Pages 2107-2116.

Blake, D.F., R.V. Morris, G. Kocurek, S.M. Morrison, R.T. Downs, D. Bish, D.W. Ming, K.S. Edgett, D. Rubin, W.Goetz, M.B. Madsen, R. Sullivan, R. Gellert, I. Campbell, A.H. Treiman, S.M. McLennan, A.S. Yen, J.Grotzinger, D.T. Vaniman, S.J. Chipera, C.N. Achilles, E.B. Rampe, D. Sumner, P.-Y. Meslin, S. Maurice, O.Forni, O. Gasnault, M. Fisk, M. Schmidt, P. Mahaffy, L.A. Leshin, D. Glavin, A. Steele, C. Freissinet, R. Navarro-González, R.A. Yingst, L.C. Kah, N. Bridges, K.W. Lewis, T.F. Bristow, J.D. Farmer, J.A. Crisp, E.M. Stolper, D.J. Des Marais, P. Sarrazin, and MSL Science Team, 2013, Curiosity at Gale Crater, Mars: Characterization and analysis of the Rocknest sand shadow, Science, 341(6153):1239505, doi:10.1126/science.1239505.

Borg, L., and Drake, M.J., 2005, A review of meteorite evidence for the timing of magmatism and of surface or near-surface liquid water on Mars, J. Geophys. Res. 110, CiteID E12S03.

Borovička J., P Spurný, P Brown, 2015, Small near-Earth asteroids as a source of meteorites, in Asteroids IV, U. Arizona Press.

Bottke, William F.; Andrews-Hanna, Jeffrey C., 2017, A post-accretionary lull in large impacts on early Mars, Nature Geoscience, Volume 10, Issue 5, pp. 344-348.

Boynton, W.V. et al., 2009. Evidence for calcium carbonate at the Mars Phoenix Landing Site. Science 325, 61–64.

Brantley, SL, & AA Olsen, 2014, Chapter 7.3: Reaction Kinetics of Primary Rock-Forming Minerals under Ambient Conditions, *in* Treatise on Geochemistry, 2nd Edition.

Bridges, J. C.; Schwenzer, S. P.; Leveille, R.; Westall, F.; Wiens, R. C.; Mangold, N.; Bristow, T.; Edwards, P.; Berger, G., 2015, Diagenesis and clay mineral formation at Gale Crater, Mars, Journal of Geophysical Research: Planets, Volume 120, Issue 1, pp. 1-19

Bristow, Thomas F.; Haberle, Robert M.; Blake, David F.; Des Marais, David J.; Eigenbrode, Jennifer L.; Fairén, Alberto G.; Grotzinger, John P.; Stack, Kathryn M.; Mischna, Michael A.; Rampe, Elizabeth B.; Siebach, Kirsten L.; Sutter, Brad; Vaniman, David T.; Vasavada, Ashwin R., 2017, Low Hesperian PCO2 constrained from in situ mineralogical analysis at Gale Crater, Mars, Proceedings of the National Academy of Sciences, vol. 114, issue 9, pp.2166-2170.

Brown P., Spalding, R. E., ReVelle, D.O., Tagliaferri, E. & S. P. Worden, The flux of small near-Earth objects colliding with the Earth, Nature 420, 294–296 (2002).

Bullock, Mark A.; Moore, Jeffrey M.; Mellon, Michael T., 2004, Laboratory simulations of Mars aqueous geochemistry, Icarus, Volume 170, Issue 2, p. 404-423.

Carr, M.H., Head, J.W., 2010. Geologic history of Mars. Earth Planet. Sci. Lett. 294, 185–203.

Carter, J., et al., 2013, Hydrous minerals on Mars as seen by the CRISM and OMEGA imaging spectrometers: Updated global view, J. Geophys. Res. Planets, 118, 831-858.

Carter, John; Loizeau, Damien; Mangold, Nicolas; Poulet, François; Bibring, Jean-Pierre, 2015, Widespread surface weathering on early Mars: A case for a warmer and wetter climate, Icarus, Volume 248, p. 373-382.

Cassata,W. et al., 2012, Trapped Ar isotopes in meteorite ALH 84001 indicate Mars did not have a thick ancient atmosphere. Earth Planet. Sci. Lett. 221, 461-465.

Catalano, Jeffrey G., 2013, Thermodynamic and mass balance constraints on iron-bearing phyllosilicate formation and alteration pathways on early Mars, Journal of Geophysical Research: Planets, Volume 118, Issue 10, pp. 2124-2136

Catling, D.C., 1999, A chemical model for evaporites on early Mars: Possible sedimentary tracers of the early climate and implications for exploration, J. Geophys. Res., doi: 10.1029/1998JE001020.

Catling, D. C., History of Mars' atmosphere, p. 66–75 *in* Gornitz, V. (ed). Encyclopedia of Paleoclimatology and Ancient Environments (Springer, 2009).

Ceplecha, Z., et al., Meteor phenomena and bodies, Space Sci. Rev. 84, 327-341 (1998).

Chambers, J.E., 1999, A Hybrid Symplectic Integrator that Permits Close Encounters between Massive Bodies, Monthly Notices of Royal Astron. Soc., 304, 793-799.

Chappelow, John E.; Golombek, Matthew P., 2010, Event and conditions that produced the iron meteorite Block Island on Mars, Journal of Geophysical Research, Volume 115, Issue E12, CiteID E00F07.

Chemtob, Steven M.; Nickerson, Ryan D.; Morris, Richard V.; Agresti, David G.; Catalano, Jeffrey G., 2017, Oxidative Alteration of Ferrous Smectites and Implications for the Redox Evolution of Early Mars, Journal of Geophysical Research: Planets, Volume 122, Issue 12, pp. 2469-2488.

Christensen, P.R., 2003, Formation of recent martian gullies through melting of extensive water-rich snow deposits, Nature, 422, 45-48.

Clarke, J.T., et al. 2014, A rapid decrease of the hydrogen corona of Mars, Geophys. Res. Lett., 41, doi:10.1002/2014FL061803.

Clow, G.D., 1987. Generation of liquid water on Mars through the melting of a dusty snowpack. Icarus 72, 95–127.

Costard, F. et al., 2002. Formation of recent martian debris flows by melting of near-surface ground ice at high obliquity. Science 295, 110–113.

Craddock, Robert A.; Lorenz, Ralph D., 2017, The changing nature of rainfall during the early history of Mars, Icarus, Volume 293, p. 172-179.

Daubar, I.J., et al., The current martian cratering rate, Icarus 225, 506-516 (2013).

Davis, P., Meteoroid impacts as seismic sources on Mars, Icarus 105, 469-478 (1993).

Dehouck, Erwin; McLennan, Scott M.; Meslin, Pierre-Yves; Cousin, Agnès., 2014, Constraints on abundance, composition, and nature of X-ray amorphous components of soils and rocks at Gale crater, Mars, Journal of Geophysical Research: Planets, Volume 119, Issue 12, pp. 2640-2657.

Dundas, Colin M.; Keszthelyi, Laszlo P.; Bray, Veronica J.; McEwen, Alfred S., 2010, Role of material properties in the cratering record of young platy-ridged lava on Mars, Geophysical Research Letters, Volume 37, Issue 12, CiteID L12203

Eberl, D. D., Farmer, V. C. & Barrer, R. M. Clay mineral formation and transformation in rocks and soils, Philos. Trans. R. Soc. Lond. A 311, 241–257 (1984).

Edwards, C. S. and B. L. Ehlmann (2015), Carbon Sequestration on Mars, Geology, doi: 10.1130/G36983.1.

Ehlmann, B. L., J. F. Mustard, S. L. Murchie, J.-P. Bibring, A. Meunier, A. A. Fraeman, and Y. Langevin (2011), Subsurface water and clay mineral formation during the early history of Mars, Nature, 479(7371), 53–60.

Ehlmann, B.L., & Edwards, C.S., 2014, Mineralogy of the Martian surface, Annual Review of Earth and Planetary Science, 42, 291-315.

Ehlmann, B., and 46 others, 2016. The Sustainability of Habitability on Terrestrial Planets: Insights, Questions, and Needed Measurements from Mars for Understanding the Evolution of Earth-like Worlds, JGR - Planets, doi: 10.1002/2016JE005134.

Elwood Madden, M., Madden, A., Rimstidt, J., 2009. How long was Meridiani Planum wet? Applying a jarosite stopwatch to constrain the duration of diagenesis. Geology 37, 635.

Fairén, Alberto G.; Davila, Alfonso F.; Gago-Duport, Luis; Haqq-Misra, Jacob D.; Gil, Carolina; McKay, Christopher P.; Kasting, James F., 2011, Cold glacial oceans would have inhibited phyllosilicate sedimentation on early Mars, Nature Geoscience, Volume 4, Issue 10, pp. 667-670.

Farley, K.A., et al., 2014, In Situ Radiometric and Exposure Age Dating of the Martian Surface, Science 343 (6169), doi: 10.1126/science.1247166.

Farrand, W. H., T. D. Glotch, and B. Horgan (2014), Detection of copiapite in the northern Mawrth Vallis region of Mars: Evidence of acid sulfate alteration, Icarus, 241(C), 346–357, doi:10.1016/j.icarus.2014.07.003.

Fassett, C.I., et al., 2010, Supraglacial and proglacial valleys on Amazonian Mars, Icarus, 208, 86-100.

Fastook, James L.; Head, James W., 2015, Glaciation in the Late Noachian Icy Highlands: Ice accumulation, distribution, flow rates, basal melting, and top-down melting rates and patterns, Planetary and Space Science, Volume 106, p. 82-98.

Forget, F. et al., 2006. Formation of glaciers on Mars by atmospheric precipitation at high obliquity. Science 311, 368–371.

Forget, F. et al., 2013. 3D modeling of the early martian climate under a dense CO2 atmosphere: Temperatures and CO2 ice clouds. Icarus. http://dx.doi.org/10.1016/j.icarus.2012.10.019.

Gainey, S. R.; Hausrath, E. M.; Hurowitz, J. A.; Milliken, R. E., 2014, Nontronite dissolution rates and implications for Mars, Geochimica et Cosmochimica Acta, Volume 126, p. 192-211.

Gibson, E. K.; Wentworth, S. J.; McKay, D. S., 1983, Chemical weathering and diagenesis of a cold desert soil from Wright Valley, Antarctica: an analog of Martian weathering processes, Journal of Geophysical Research, Vol. 88, Suppl., p. A912 - A928.

Golombek, M. P.; Grant, J. A.; Crumpler, L. S.; Greeley, R.; Arvidson, R. E.; Bell, J. F.; Weitz, C. M.; Sullivan, R.; Christensen, P. R.; Soderblom, L. A.; Squyres, S. W., 2006, Erosion rates at the Mars Exploration Rover landing sites and long-term climate change on Mars, Journal of Geophysical Research 111, Issue E12, CiteID E12S10.

Golombek, M., et al., 2010, Constraints on ripple migration at Meridiani Planum from Opportunity and HiRISE observations of fresh craters. Journal of Geophysical Research (Planets), 115, E00F08, doi:10.1029/2010JE003628.

Golombek, M., et al., 2014, Small crater modification on Meridiani Planum and implications for erosion rates and climate change on Mars, J. Geophys. Res., doi:10.1002/2014JE004658.

Grant, J.A., & Wilson, S.A., 2011, Late alluvial fan formation in southern Margaritifer Terra, Mars, Geophys. Res. Lett. 38, CiteID L08201.

Grant, J.A., & Wilson, S.A., 2012, A possible synoptic source of water for alluvial fan formation in southern Margaritifer Terra, Mars, Planetary and Space Science, 72, 44-52.

Gröller, H., et al., Hot oxygen and carbon escape from the martian atmosphere, Planetary and Space Sci., 98, 93-105.

Grotzinger, J., Beaty, D., Dromart, G., Gupta, S., Harris, M., Hurowitz, J., Kocurek, G., McLennan, S., Milliken, R., Ori, G.G., & Sumner D., 2011, Mars Sedimentary Geology:

Key Concepts and Outstanding Questions, Astrobiology. 11(1): 77-87. doi:10.1089/ast.2010.0571.

Grotzinger, J.P., Milliken, R.E., 2012. The sedimentary rock record of Mars: Distribution, origins, and global stratigraphy. In: Grotzinger, J.P. (Ed.), Sedimentary Geology of Mars, Special Publications, vol. 102. SEPM (Society for Sedimentary Geology), pp. 1–48

Grotzinger, J.P., et al., 2014, A habitable fluvio-lacustrine environment at Yellowknife Bay, Gale Crater, Mars, Science 343, doi:10.1126/science.1242777.

Haberle, R.M., 1998. Early Mars climate models. J. Geophys. Res. 1032, 28467–28480.

Haberle R.M., et al., 2017, The Early Mars Climate System, in Haberle, Robert M.; Clancy, R. Todd; Forget, F.; Smith, Michael D.; Zurek, Richard W. (Eds)., The atmosphere and climate of Mars, Edited by R.M. Haberle et al. ISBN: 9781139060172. Cambridge University Press, 2017

Halevy, I.; Fischer, W. W.; Eiler, J. M., 2011, Carbonates in the Martian meteorite Allan Hills 84001 formed at 18 4 C in a near-surface aqueous environment, Proceedings of the National Academy of Sciences, vol. 108, issue 41, pp. 16895-16899

Halevy, I., and Head, J.W., 2014, Episodic warming of early Mars by punctuated volcanism, Nature Geoscience, doi:10.1038/NGEO2223.

Hartmann, W. K., 2005, Martian cratering 8: Isochron refinement and the chronology of Mars, Icarus, 174, 294–320.

Hartmann, W. K.; Daubar, I. J., 2017, Martian cratering 11. Utilizing decameter scale crater populations to study Martian history, Meteoritics & Planetary Science, Volume 52, Issue 3, pp. 493-510.

Hecht, M.H., 2002. Metastability of liquid water on Mars. Icarus 156, 373–386.

Hobbs, K. M. & Parrish, J. T., 2016, Miocene global change recorded in Columbia River basalt-hosted paleosols. Geol. Soc. Am. Bull. 128, 1543–1554.

Holsapple, K.A., 1993, The scaling of impact processes in planetary sciences, Ann. Rev. Earth Planet. Sci. 21, 333-373.

Horgan, B., J. A. Kahmann-Robinson, J. L. Bishop, and P. R. Christensen (2013), Climate Change and a Sequence of Habitable Ancient Surface Environments Preserved in Pedogenically Altered Sediments at Mawrth Vallis, Mars, 44th Lunar and Planetary Science Conference, 1719, 3059.

Horgan, B., D. Loizeau, F. Poulet, J. Bishop, N. Mangold, 2017a, Origin and astrobiological potential of ancient surface and subsurface environments at Mawrth Vallis. 3rd landing site workshop for the 2020 Mars Rover mission, https://marsnext.jpl.nasa.gov/workshops/wkshp_2017_02.cfm.

Horgan, B.; Baker, L.; Carter, J.; Chadwick, O., 2017b, Where is the Climate Signature in the Mineral Record of Early Mars? Fourth International Conference on Early Mars: Geologic, Hydrologic, and Climatic Evolution and the Implications for Life, Proceedings of the conference held 2-6 October, 2017 in Flagstaff, Arizona. LPI Contribution No. 2014, 2017, id.3077.

Horgan, B., R. Smith*, P. Mann, E. Cloutis, P. Christensen (2017). Acid weathering of basalt and basaltic glass: I. Near-infrared spectra, mid-infrared spectra, and implications for Mars, Icarus, doi:10.1002/2016JE005111

Hu, Renyu; Kass, David M.; Ehlmann, Bethany L.; Yung, Yuk L., 2015, Tracing the fate of carbon and the atmospheric evolution of Mars, Nature Communications, Volume 6, id. 10003.

Hudson, T.L., Aharonson, O., 2008. Diffusion barriers at Mars surface conditions: Salt crusts, particle size mixtures, and dust. J. Geophys. Res. 113, E09008.

Hynek, Brian, 2016, The great climate paradox of ancient Mars, Geology, vol. 44, issue 10, pp. 879-880.

Hynek, B.M., and Di Achille, G., 2017, Geologic map of Meridiani Planum, Mars (ver. 1.1, April 2017): U.S. Geological Survey Scientific Investigations Map 3356, pamphlet 9 p., scale 1:2,000,000, https://doi.org/10.3133/sim3356.

Ingersoll, A.P., 1970, Mars: occurrence of liquid water, Science, 168, 972-973.

Irwin, R.P., Lewis, K.W., Howard, A.D., and Grant, J.A., 2015, Paleohydrology of Eberswalde crater, Mars, Geomorphology, doi:10.1016/j.geomorph.2014.10.012.

Jakosky, B.M., & Phillips, R.J., 2001, Mars' volatile and climate history, Nature, 412, 237-244.

JeongAhn, Y., Malhotra, R., 2015, The current impact flux on Mars and its seasonal variation, Icarus, 262, p. 140-153

Jerolmack, D.J., & Sadler, P., 2007, Transience and persistence in the depositional record of continental margins, J. Geophys. Res. – Earth Surface, 112, F3, DOI:10.1029/2006JF000555.

Jerolmack, Douglas J., and Chris Paola, 2010, Shredding of environmental signals by sediment transport, Geophys. Res. Lett., doi: 10.1029/2010GL044638.

Johnson, A.P., et al., 2011, Extended survival of several organisms and amino acids under simulated martian surface conditions, Icarus, 211, 1162-1178.

Kahn, R. 1985, The evolution of CO2 on Mars, Icarus, 62, 175.

Kanzaki, Yoshiki; Murakami, Takashi, 2015, Estimates of atmospheric CO2 in the Neoarchean-Paleoproterozoic from paleosols, Geochimica et Cosmochimica Acta, Volume 159, p. 190-219.

Kite, E.S., et al., 2009, True polar wander driven by late-stage volcanism and the distribution of paleopolar deposits on Mars, Earth and Planet. Sci. Lett. 280, 254-267.

Kite, E.S.; Michaels, Timothy I.; Rafkin, Scot; Manga, Michael; Dietrich, William E., 2011a, Localized precipitation and runoff on Mars, Journal of Geophysical Research, Volume 116, Issue E7, CiteID E07002

Kite, E.S., Gaidos, E., and Manga, M., 2011b, Climate instability on tidally locked exoplanets, Astrophys. J., 743, article id 41, 12 pp.

Kite, E.S., Rafkin, S.C.R., Michaels, T.I., Dietrich, W.E., & Manga, M., 2011c, Chaos terrain, storms, and past climate on Mars, J. Geophys. Res. – Planets, 116, E10002, 26 pp., doi:10.1029/2010JE003792.

Kite, E.S., Lucas, A., & C.I. Fassett, 2013b. Pacing Early Mars river activity: Embedded craters in the Aeolis Dorsa region imply river activity spanned ≳(1–20) Myr, Icarus, 225, 850-855.

Kite, E.S., Howard, A., Lucas, A., Armstrong, J.C., Aharonson, O., & Lamb, M.P., 2014b, Stratigraphy of Aeolis Dorsa, Mars: resolving the great drying of Mars, Lunar and Planetary Science Conference, astract number 2638.

Kite, E.S., Williams, J.-P., Lucas, A., & Aharonson, O., 2014a, Paleopressure of Mars' atmosphere from small ancient craters, Nature Geoscience, 7, 335-339.

Kite, E.S., Howard, A., & Lucas, A., 2015a, "Resolving the era of river-forming climates on Mars using stratigraphic logs of river-deposit dimensions," *EPSL*, 420, 55-65.

Kite, E.S., Howard, A., Lucas, A., Armstrong, J., Aharonson, O., & Lamb, M., 2015b, "Stratigraphy of Aeolis Dorsa, Mars: sequencing the great river deposits," *Icarus,* 253, 223-242.

Kite, E.S., Sneed, J., Mayer, D.P., & Wilson, S.A., 2017. "Persistent or repeated surface habitability on Mars," Geophysical Research Letters, 44, 3991-3999.

Kite, E.S., & Ford, E., "Habitability of exoplanet waterworlds," arXiv:1801.00748.

Kloprogge, J. T., Komarneni, S. & Amonette, J. Synthesis of smectite clay minerals: a critical review. Clays Clay Miner. 47, 529–554 (1999).

Knoll, A.H., et al., 2008, Veneers, rinds, and fracture fills: Relatively late alteration of sedimentary rocks at Meridiani Planum, Mars. Journal of Geophysical Research, Volume 113, Issue E6, CiteID E06S16.

Kopparapu, R.K., et al., 2013, Habitable zones around main-sequence stars: New estimates, Astrophys. J., 765, articl id. 131, 16 pp.

Kreslavsky, M. A., 2011, Observational Constraints on atmospheric Pressure on Mars in the Amazonian, The Fourth International Workshop on the Mars Atmosphere: Modelling and observation, held 8-11 February, 2011, in Paris, France. Published online at http://www-mars.lmd.jussieu.fr/paris2011/program.html, pp.443-446.

Kreslavsky, M.A., and Head, J.W., 2005, Mars at very low obliquity: Atmospheric collapse and the fate of volatiles, Geophys. Res. Lett., 32, CiteID L12202.

Lapôtre, M. G. A., et al. (2016), Large wind ripples on Mars: A record of atmospheric evolution, Science, 353, 55–58.

Laskar, J., et al., 2004, Long term evolution and chaotic diffusion of the insolation quantities of Mars, Icarus 170, 343-364.

Lee, Yong Il; Lim, Hyoun Soo; Yoon, Ho Il, 2004, Geochemistry of soils of King George Island, South Shetland Islands, West Antarctica: Implications for pedogenesis in cold polar regions, Geochimica et Cosmochimica Acta, Volume 68, Issue 21, p. 4319-4333.

Leshin, L.A., et al., 2013, Volatile, isotope and organic analysis of Martian fines with the Mars Curiosity rover, Science, 341, id. 1238937.

Lewis, K.W. et al., 2008. Quasi-periodic bedding in the sedimentary rock record of Mars, Science 322, 1532–1535

Lewis, K., and Aharonson, O., 2014, Occurrence and origin of rhythmic sedimentary rocks on Mars, J. Geophys. Res. Planets 119, 1432-1457.

Lillis, Robert J.; Deighan, Justin; Fox, Jane L.; Bougher, Stephen W.; Lee, Yuni; Combi, Michael R.; Cravens, Thomas E.; Rahmati, Ali; Mahaffy, Paul R.; Benna, Mehdi; Elrod, Meredith K.; McFadden, James P.; Ergun, Robert. E.; Andersson, Laila; Fowler, Christopher M.; Jakosky, Bruce M.; Thiemann, Ed; Eparvier, Frank; Halekas, Jasper S.; Leblanc, François; Chaufray, Jean-Yves, 2017, Photochemical escape of oxygen from Mars: First results from MAVEN in situ data, Journal of Geophysical Research: Space Physics, Volume 122, Issue 3, pp. 3815-3836.

Lissauer, J.J., Barnes, J.W., and Chambers, J.E., Obliquity variations of a moonless Earth, Icarus, 217, p. 77-87.

Loizeau, D.; Mangold, N.; Poulet, F.; Ansan, V.; Hauber, E.; Bibring, J.-P.; Gondet, B.; Langevin, Y.; Masson, P.; Neukum, G., 2010, Stratigraphy in the Mawrth Vallis region through OMEGA, HRSC color imagery and DTM, Icarus, Volume 205, Issue 2, p. 396-418.

Loizeau, D., et al., 2012, Chronology of deposition and alteration in the Mawrth Vallis region, Mars, Planetary and Space Science, 72, 31-43.

Loizeau, D.; Mangold, N.; Poulet, F.; Bibring, J.-P.; Bishop, J. L.; Michalski, J.; Quantin, C., 2015, History of the clay-rich unit at Mawrth Vallis, Mars: High-resolution mapping of a candidate landing site, Journal of Geophysical Research: Planets, Volume 120, Issue 11, pp. 1820-1846.

Lundin, R., et al., 2013, Solar cycle effects on the ion escape from Mars, Geophys. Res. Lett., 40, 6028-6032.

Madeleine, J.-B. et al., 2009. Amazonian northern mid-latitude glaciation on Mars: A proposed climate scenario. Icarus 203, 390–405.

Madeleine, J.-B., 2014, Recent ice ages on Mars: The role of radiatively active clouds and cloud microphysics, Geophys. Res. Lett. 41, 4873-4879.

Maher, K.; Chamberlain, C. P., 2014, Hydrologic Regulation of Chemical Weathering and the Geologic Carbon Cycle, Science, Volume 343, Issue 6178, pp. 1502-1504.

Malin, M.C. and Edgett, K.S., 2000, Sedimentary Rocks of Early Mars. Science, 290,1927-1937, doi:10.1126/science.290.5498.1927.

Manga, M., Patel, A., Dufek, J. & Kite, E. S. Wet surface and dense atmosphere on early Mars inferred from the bomb sag at Home Plate, Mars. Geophys. Res. Lett. 39, L01202 (2012)

Manning, C., McKay, C.P., and Zahnle, K.J., 2006, Thick and thin models of the evolution of carbon dioxide on Mars, Icarus, 180, 38-59.

Mansfield, M., Kite, E.S., & Mischna, M., "Effect of Mars atmospheric loss on snow melt potential in a 3.5-Gyr climate evolution model," in press at JGR-Planets.

McAdam, Amy C.; Franz, Heather B.; Sutter, Brad; Archer, Paul D.; Freissinet, Caroline; Eigenbrode, Jennifer L.; Ming, Douglas W.; Atreya, Sushil K.; Bish, David L.; Blake, David F.; Bower, Hannah E.; Brunner, Anna; Buch, Arnaud; Glavin, Daniel P.; Grotzinger, John P.; Mahaffy, Paul R.; McLennan, Scott M.; Morris, Richard V.; Navarro-González, Rafael; Rampe, Elizabeth B.; Squyres, Steven W.; Steele, Andrew; Stern, Jennifer C.; Sumner, Dawn Y.; Wray, James J., 2014, Sulfur-bearing phases detected by evolved gas analysis of the Rocknest aeolian deposit, Gale Crater, Mars, Journal of Geophysical Research: Planets, Volume 119, Issue 2, pp. 373-393.

McDonald, Eric, and Alan J. Busacca, 1990, Interaction between aggrading geomorphic surfaces and the formation of a late pleistocene paleosol in the palouse loess of eastern Washington state, Geomorphology, Volume 3, Issues 3–4, September 1990, Pages 449-469, https://doi.org/10.1016/0169-555X(90)90016-J

McEwen, A.S., & Bierhaus, E.B., The importance of secondary cratering to age constraints on planetary surfaces, Annual Review of Earth and Planetary Sciences 34, 535-567 (2006).

McEwen, A.S., et al. 2014, Recurring slope lineae in equatorial regions of Mars, Nature Geosci., 7, 53-58.

McKay, C.P., Wharton, R.A. Jr., Squyres, S.W., & Clow, G.D., 1985, Thickness of ice on perennially frozen lakes, Nature, 313, 561-562.

Melosh, J., 1989, Impact cratering: a geologic process, Oxford University Press.

Melwani Daswani, M., & Kite, E.S., 2017. Paleohydrology on Mars constrained by mass balance and minerology of pre-Amazonian sodium chloride lakes: Deep groundwater not required, JGR – Planets, 122, 1802-1823.

Michael, G.G., 2013, Planetary surface dating from crater size-frequency distribution measurements: multiple resurfacing episodes and differential isochron fitting, Icarus, 226 (1) (2013), pp. 885-890

Michael, G. G.; Kneissl, T.; Neesemann, A., 2016, Planetary surface dating from crater size-frequency distribution measurements: Poisson timing analysis, Icarus, Volume 277, p. 279-285.

Michalski, J.R. and Niles, P.B., 2012, An atmospheric origin of Martian Interior Layered Deposits (ILDs): Links to climate change and the global sulfur cycle. Geology, 40, 419-422, doi:10.1130/G32971.1.

Milliken, R.E., et al., 2008, Opaline silica in young deposits on Mars, Geology 36, 847-850.

Milliken, R. E.; Fischer, W. W.; Hurowitz, J. A., 2009, Missing salts on early Mars, Geophysical Research Letters, Volume 36, Issue 11, CiteID L11202.

Milliken, R. E.; Ewing, R. C.; Fischer, W. W.; Hurowitz, J., 2014, Wind-blown sandstones cemented by sulfate and clay minerals in Gale Crater, Mars, Geophysical Research Letters 41, 1149-1154.

Nezat, Carmen A.; Lyons, W. Berry; Welch, Kathleen A., 2001, Chemical weathering in streams of a polar desert (Taylor Valley, Antarctica), Geological Society of America Bulletin, 113, 1401-1408.

Niles, P.B., et al., 2013, Geochemistry of Carbonates on Mars: Implications for Climate History and Nature of Aqueous Environments, Space Sci. Rev., 174, 301-328.

Noe Dobrea, E. Z.; Bishop, J. L.; McKeown, N. K.; Fu, R.; Rossi, C. M.; Michalski, J. R.; Heinlein, C.; Hanus, V.; Poulet, F.; Mustard, R. J. F.; Murchie, S.; McEwen, A. S.; Swayze, G.; Bibring, J.-P.; Malaret, E.; Hash, C., 2010, Mineralogy and stratigraphy of phyllosilicate-bearing and dark mantling units in the greater Mawrth Vallis/west Arabia Terra area: Constraints on geological origin, Journal of Geophysical Research, Volume 115, Issue E11, CiteID E00D19.

Noe Dobrea, Eldar Z.; Michalski, Joseph; Swayze, Gregg, 2011, Aqueous mineralogy and stratigraphy at and around the proposed Mawrth Vallis MSL Landing Site: New insights into the aqueous history of the region, Mars: The International Journal of Mars Science and Exploration Volume 6, p. 32-46

Paige, D. A.; Golombek, M. P.; Maki, J. N.; Parker, T. J.; Crumpler, L. S.; Grant, J. A.; Williams, J. P., 2007, MER Small Crater Statistics: Evidence Against Recent Quasi-Periodic Climate Variations, Seventh International Conference on Mars, held July 9-13, 2007 in Pasadena, California, LPI Contribution No. 1353, p.3392.

Palucis, M.C., et al., 2014, The origin and evolution of the Peace Vallis fan system that drains to the Curiosity landing area, Gale Crater, Mars, J. Geophys. Res., 199, 705-728.

Pepin, R.O., 1994, Evolution of the martian atmosphere, Icarus 111, 289-304.

Peretyazhko, T. S.; Niles, P. B.; Sutter, B.; Morris, R. V.; Agresti, D. G.; Le, L.; Ming, D. W., 2018, Smectite formation in the presence of sulfuric acid: Implications for acidic smectite formation on early Mars, Geochimica et Cosmochimica Acta, Volume 220, p. 248-260.

Pierazzo, E., & H.J. Melosh, Understanding oblique impacts from experiments, observations, and modeling, Annu. Rev. Earth Planet. Sci. 28, 141-168 (2000).

Pierrehumbert, R.P., 2010, Principles of planetary climate, Cambridge University Press.

Phillips, R.J., et al., Ancient geodynamics and global-scale hydrology on Mars, Science, 291, 2587-2591.

Phillips, R.J., et al., 2011, Massive CO_2 ice deposits sequestered in the south polar layered deposits of Mars, Science, 332, 838-.

Pollack, J.B., et al., 1987, The case for a wet, warm climate on early Mars, Icarus, 71, 203-224.

Putzig, N.E., et al., 2009, Subsurface structure of Planum Boreum from Mars Reconnaissance Orbiter Shallow Radar soundings, Icarus, 204, 443-457.

Quinn, R., Zent, A.P., and McKay, C.P., 2006, Photochemical stability of carbonates on Mars, Astrobiology, 6, 581-591.

Reed, M.H., 1982, Calculation of multicomponent chemical equilibria and reaction processes in systems involving minerals, gases and an aqueous phase, Geochim. Cosmochim. Acta 46, 513-528.

Reed, M. H. (1998), Calculation of simultaneous chemical equilibria in aqueous-mineral-gas systems and its application to modeling hydrothermal processes, in Techniques in Hydrothermal Ore Deposits Geology, Reviews in Economic Geology, vol. 10, edited by J. P. Richards and P. B. Larson, pp. 109–124, Society of Economic Geologists, Littleton, Colo.

Retallack, G. J., E. A. Bestland, and T. J. Fremd (2000), Eocene and Oligocene paleosols of central Oregon, GSA Special Papers, 344, 1–192.

Robbins, S.J., 2014, New crater calibrations for the lunar crater-age chronology, Earth and Planet. Sci. Lett. 403, 188-198.

Robbins, Stuart J., Jamie D. Riggs, Brian P. Weaver, Edward B. Bierhaus, Clark R. Chapman, Michelle R. Kirchoff, Kelsi N. Singer, Lisa R. Gaddis, 2018, Revised recommended methods for analyzing crater size-frequency distributions, Meteoritics & Planetary Science, DOI: 10.1111/maps.12990.

Schieber, J., Bish, D., Coleman, M., Reed, M., Hausrath, E. M., Cosgrove, J., Gupta, S., Minitti, M. E., Edgett, K. S. and Malin, M. (2017), Encounters with an unearthly mudstone: Understanding the first mudstone found on Mars. Sedimentology, 64: 311–358. doi:10.1111/sed.12318.

Schwenzer, S. P.; Bridges, J. C.; Wiens, R. C.; Conrad, P. G.; Kelley, S. P.; Leveille, R.; Mangold, N.; Martín-Torres, J.; McAdam, A.; Newsom, H.; Zorzano, M. P.; Rapin, W.; Spray, J.; Treiman, A. H.; Westall, F.; Fairén, A. G.; Meslin, P.-Y., 2016, Fluids during diagenesis and sulfate vein formation in sediments at Gale crater, Mars, Meteoritics & Planetary Science, Volume 51, Issue 11, pp. 2175-2202.

Sheldon, Nathan D.; Tabor, Neil J., 2009, Quantitative paleoenvironmental and paleoclimatic reconstruction using paleosols, Earth Science Reviews, Volume 95, Issue 1, p. 1-52.

Siebach, K. L.; Baker, M. B.; Grotzinger, J. P.; McLennan, S. M.; Gellert, R.; Thompson, L. M.; Hurowitz, J. A., 2017, Sorting out compositional trends in sedimentary rocks of the Bradbury group (Aeolis Palus), Gale crater, Mars, Journal of Geophysical Research: Planets, Volume 122, Issue 2, pp. 295-328.

Soto, A., M. Mischna, T. Schneider, C. Lee, and M. Richardson (2015), Martian atmospheric collapse: Idealized GCM studies. Icarus, doi:10.1016/j.icarus.2014.11.028

Squyres, S.W., and Kasting, J.F., 1994, Early Mars: How warm and how wet?, Science 265, 744-749.

Squyres, S.W., and the Athena Science Team, 2012, Ancient Impact and Aqueous Processes at Endeavour Crater, Mars. Science, 336 (6081), 570-576, doi:10.1126/science.1220476.

Strom, Robert G.; Malhotra, Renu; Ito, Takashi; Yoshida, Fumi; Kring, David A., 2005, The Origin of Planetary Impactors in the Inner Solar System, Science, Volume 309, Issue 5742, pp. 1847-1850.

Summons, R.E., 2011, Preservation of Martian Organic and Environmental Records: Final Report of the Mars Biosignature Working Group, Astrobiology, 11, 157-181.

Thomson, B.J., et al., 2011, Constraints on the origin and evolution of the layered mound in Gale Crater, Mars using Mars Reconnaissance Orbiter data. Icarus, 214, 413 – 432.

Toon, O.B., et al., 1980, The astronomical theory of climatic change on Mars, Icarus, 44, 552-607.

Tosca, Nicholas J.; Knoll, Andrew H., 2009, Juvenile chemical sediments and the long term persistence of water at the surface of Mars, Earth and Planetary Science Letters, Volume 286, Issue 3-4, p. 379-386.

Tosca, N. J.; Ahmed, I.; Ashpitel, A.; Hurowitz, J. A., 2017, Magnetite Authigenesis and the Ancient Martian Atmosphere, Fourth International Conference on Early Mars: Geologic, Hydrologic, and Climatic Evolution and the Implications for Life, Proceedings of the conference held 2-6 October, 2017 in Flagstaff, Arizona. LPI Contribution No. 2014, 2017, id.3015.

Tréguier, Erwan; d'Uston, Claude; Pinet, Patrick C.; Berger, Gilles; Toplis, Michael J.; McCoy, Timothy J.; Gellert, Ralf; Brückner, Johanne, 2008, Overview of Mars surface geochemical diversity through Alpha Particle X-Ray Spectrometer data multidimensional analysis: First attempt at modeling rock alteration, Journal of Geophysical Research, Volume 113, Issue E12, CiteID E12S34.

van Berk,W., Fu, Y. & Ilger, J-M. Reproducing early martian atmospheric carbon dioxide partial pressure by modeling the formation of Mg/Fe/Ca carbonate identified in the Comanche rock outcrops on Mars. J. Geophys. Res.117, E10008 (2012)

Vasavada, A. R., Milavec, T. J. & Paige, D. A. Microcraters on Mars: Evidence for past climate variations. J. Geophys. Res. 98, 3469-3476 (1993).

Vasavada, Ashwin R., 2017, Our changing view of Mars, Physics Today, vol. 70, issue 3, pp. 34-41.

Velde, B., 1995, Origin and Mineralogy of Clays: Clays and the Environment, Springer.

Velde, B., and Meunier, A., 2008, The Origin of Clay Minerals in Soils and Weathered Rocks, Springer.

Wall, J.V. & Jenkins, C.R., Practical statistics for astronomers, 2nd Edition (Cambridge Observing Handbooks for Research Astronomers), Cambridge University Press, Cambridge, UK (2012).

Walker, J.C.G., Hays, P.B., and Kasting, J.F., A negative feedback mechanism for the long-term stabilization of the earth's surface temperature, J. Geophys. Res., 86, 9776-9782.

Warner, N., Gupta, S., Calef, F., Grindrod, P., Boll, N., and Goddard, K., 2015, Minimum effective area for high resolution crater counting of Martian terrains, Icarus, 245, 198-240.

Watters, W. A., L. M. Geiger, M. Fendrock, and R. Gibson (2015), Morphometry of small recent impact craters on Mars: Size and terrain dependence, short-term modification. J. Geophys. Res. Planets, 120, 226–254. doi: 10.1002/2014JE004630.

Webster, C.R., et al., 2015, Isotope Ratios of H, C, and O in CO2 and H2O of the Martian Atmosphere, Science 341, 260-263.

White, AF, & HL Buss, Chapter 7.4: Natural Weathering Rates of Silicate Minerals, *in* Treatise on Geochemistry, 2nd Edition.

Wordsworth, R.D., Kerber, L., Pierrehumbert, R.T., Forget, F., and Head, J.W., 2015, Comparison of "warm and wet" and "cold and icy" scenarios for early Mars in a 3-D climate model, J. Geophys. Res. – Planets, 120(6), 1201-1219.

Williams, J.-P., van der Bogert, C. H., Pathare, A. V., Michael, G. G., Kirchoff, M. R. and Hiesinger, H., 2017, Dating very young planetary surfaces from crater statistics: A review of issues and challenges. Meteorit Planet Sci. doi:10.1111/maps.12924

Williams, Jean-Pierre; Pathare, Asmin V.; Aharonson, Oded, 2014, The production of small primary craters on Mars and the Moon, Icarus, Volume 235, p. 23-36.

Winnick, Matthew J.; Maher, Kate, 2018, Relationships between CO2, thermodynamic limits on silicate weathering, and the strength of the silicate weathering feedback, Earth and Planetary Science Letters, Volume 485, p. 111-120.

Zolotov, Mikhail Yu.; Mironenko, Mikhail V., 2016, Chemical models for martian weathering profiles: Insights into formation of layered phyllosilicate and sulfate deposits, Icarus, Volume 275, p. 203-220.

Zuber, M.T., et al., 2007, Density of Mars' South Polar Layered Deposits, Science, 317, 1718-.